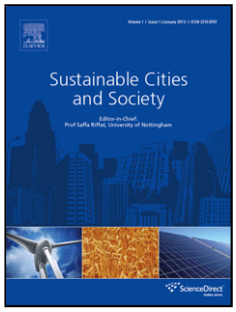

Title: A comparison of battery and phase change coolth storage in a PV cooling system under different climates

Authors: Xiaolin Wang, Mike Dennis

PII: S2210-6707(17)30611-X
DOI: https://doi.org/10.1016/j.scs.2017.09.035
Reference: SCS 789

To appear in:

Received date: 2-6-2017
Revised date: 28-9-2017
Accepted date: 28-9-2017

Please cite this article as: Wang, Xiaolin., & Dennis, Mike., A comparison of battery and phase change coolth storage in a PV cooling system under different climates.*Sustainable Cities and Society* https://doi.org/10.1016/j.scs.2017.09.035

A comparison of battery and phase change coolth storage in a PV cooling system under different climates

Xiaolin Wang, Mike Dennis

Research School of Engineering, the Australian National University, Canberra 0200, Australia

Corresponding author: Xiaolin Wang, xiaolin.wang@anu.edu.au

Highlights

1. A coolth storage component was modelled with CO_2 gas hydrate as the PCM.

2. The energy savings of coolth storage and battery in a PV cooling system were compared.

3. The influencing factors on the charge and discharge of energy storage were analysed.

4. The performance of PV-battery was found better than that of PV-coolth storage cooling system.

Abstract: Energy storage in PV cooling systems is desirable to supply on-site loads during solar outages. Current storage methods of such systems typically use battery storage to store surplus electricity generated by solar panels or coolth thermal energy storage (CTES) to store excess cooling capacity produced by an electric-driven chiller. This study compares three cooling system configurations – no energy storage, with a battery storage, and with a phase change CTES, for a residential building under the climate of Shanghai, Madrid and Brisbane.

Corresponding author: Xiaolin Wang, xiaolin.wang@anu.edu.au

System simulation of each configuration was conducted using TRNSYS. A CTES component was programmed externally using effectiveness-NTU method. Both energy storage methods were compared with regard to energy change during a summer day, power consumption and primary energy saving ratio (PESR) during the cooling season. In addition, performance of a single battery and a single CTES were evaluated under various operational conditions. The results showed good energy performance of both storage cases. The PESR of battery case and coolth storage case were 2.8 times and 1.9 times higher than that of a reference case with no energy storage.

Keywords: *PV cooling; battery; phase change coolth storage; primary energy saving*

Nomenclature

ε	*heat exchanger effectiveness*
δ	*phase change fraction*
U	*overall heat-transfer coefficient, W/(m^2·K)*
A	*heat transfer area, m^2*
$\dot{m}$	*mass flow rate of HTF, kg/s*
C_p	*specific heat of the HTF, kJ/(kg·K)*
L	*tube length, m*
R_i	*inner radius of the tube, m*
R_o	*outer radius of the tube, m*
R_{max}	*max radius of frozen PCM between phase change interface of adjacent tubes, m*
R_T	*total thermal resistance, K/W*
R_{HTF}	*thermal resistance of the HTF, K/W*
R_{WALL}	*thermal resistance of the tube wall, K/W*
R_{PCM}	*thermal resistance of the PCM, K/W*
h_{HTF}	*heat transfer coefficient of the HTF, W/(m^2·K)*
k_{WALL}	*thermal conductivity of the tube wall, W/(m·K)*
k_{PCM}	*thermal conductivity of PCM, W/(m·K)*
T_i	*coolth storage inlet HTF temperature, ^{o}C*
T_o	*coolth storage outlet HTF temperature, ^{o}C*
T_{PCM}	*phase change temperature, ^{o}C*

1 Background

Space cooling over summer periods has been a contributing factor to the increasing power consumption and grid load over the past decades. This is mainly due to the prevalent use of air conditioning system with the mechanical vapour compression refrigeration cycle. To alleviate

peak grid load, photovoltaic (PV) powered cooling systems are being widely implemented and studied [1–3]. Such systems use PV arrays as a primary generation source that converts solar energy into electricity when operates synchronously and in parallel with electricity grids, and drives the HVAC chiller to meet cooling demand with electricity grid as a backup. PV cooling has demonstrated advantages over other solar-driven cooling systems. A simulation work comparing a PV cooling system and a solar thermal cooling system was conducted under different climates [4]. By evaluating energy saving performance of both systems, it was shown that the energy efficiency of PV cooling was obviously higher. It accounted for almost half of the energy demand with a primary energy saving of 50%.

It is undeniable that power supply through PV techniques can offset grid load to a large extent, however solar energy has intrinsic intermittency that may frequently lead to of power outage. Energy storage has been proven favourable in supplying on-site loads during solar outages and peak load hours. For PV cooling systems, current storage methods typically use electricity storage to store surplus electricity by generated solar panels, or coolth thermal energy storage (CTES) to conserve excess cooling capacity produced by a chiller in the form of sensible or latent heat. For electricity storage, the significance of a sizable PV/battery system in reducing marginal prices and grid power supply has been verified [5]. The grid and PV charged the battery at midnight and early morning hours respectively when hourly loads are relatively low. The fact that a higher power (6.24 MW) was required to charge the battery (4.68 MW) reveals the efficiency of the battery was 75%. The application of the PV/battery unit saved 2.8% of the daily thermal generation cost for the load (reduced from $41,822.02 to $40,670.16). Compared with battery storage, coolth thermal storage is a burgeoning technology that has sprouted many investigations. Using a TRNSYS model, the energy efficiency of a residential cooling system with a cold water thermal storage was predicted under the climate of Spain, in contrast with configurations with a hot water thermal storage or without any energy storage [6]. The results showed a better performance in the case of cold water store, especially when the store's size was large while the solar collector area was small. A domestic-scale prototype solar cooling system was developed, which consists of solar collectors, a LiBr/H_2O absorption chiller and a cold water storage [7]. The average coefficient of system thermal performance was 0.58 in, based on a 12 m^2 collector on a hot sunny day with the average peak insolation of 800 W/m^2 and ambient temperature of 24^{o}C. In another work, the viability of a sensible cold water storage was studied when the chilled water temperature was 7.4 ℃ [8]. These studies all demonstrated the potential of sensible coolth storage using cold water in HVAC systems.

Compared with sensible thermal energy storage materials such as water and salt, phase change material (PCM) can store more thermal energy by per unit volume in the form of latent heat

with particular reference to off-peak thermal storage applications [9, 10]. The model in this study will be built on a phase change CTES.

Both battery and CTES are capable of conserving sufficient energy for later use and deliver high energy savings by intensively utilizing available solar energy. This study will present a simulation work using TRNSYS to investigate the performance of a PV cooling system with a lead-acid battery and a PCM CTES, respectively, for a residential building under the climates of Brisbane, Madrid and Shanghai. For coolth storage, CO_2 gas hydrate will be employed as the PCM for its suitable phase change temperature and large latent heat in a limited volume [11–15]. The CTES will be programmed externally using thermal properties of the CO_2 gas hydrate material. The power consumption and the primary energy saving ratio (PESR) of the battery/CTES based PV cooling system will be evaluated during a one-day operation and a cooling season operation. In addition, the energy performance of a single electricity storage and a single coolth thermal energy storage under various conditions will be examined.

2 Simulation background

2.1 Building and climate description

A multi-zone residential building with a total conditioned area of 196.1 m^2 is compiled in the model. Details of zones are in Table 1 [16]. Cooling demand during scheduled ventilation period (6:00–9:00 AM and 5:00–10:00 PM) is inputted to the system simulation with the user profile and building structures the same for all cases. The simulation is conducted using weather files of Shanghai, Madrid and Brisbane. In the cooling season of Shanghai and Madrid (July, August and September), the cooling load (including the sensible and latent load) is 9940 kWh and 7930 kWh, respectively. In Brisbane, during the cooling season (December, January and February) the cooling load accumulates to 9510 kWh. The average daily solar radiation of Shanghai, Madrid and Brisbane is 0.37, 0.43 and 0.46 kW/m^2, respectively.

2.2 System configuration

Three cases are built in the model – a reference case, a battery storage (BS) case and a coolth storage (CS) case (Figure 1). The HVAC chillers in three cases are of the same size. In the BS and CS case, PV modules are connected to an electric-driven chiller via a DC/AC inverter. The reference case (a) has no energy storage and its power consumption is totally shoulder by electricity grid. In the BS case (b), a battery is connected to the inverter to charge electricity from PV modules when solar energy is sufficient, and to discharge electricity during outages. In the CS case (c), a coolth storage tank is placed in parallel with air conditioning terminals (fan-coils). In the charge, electricity from PV modules is directly used to drive the chiller to

produce cooling capacity to cool the primary chilled water. The primary chilled water is then circulated to the coolth storage tank and freezes the PCM inside. In the discharge, cooling capacity is released by melting the PCM to cool down the secondary chilled water. The secondary chilled water is finally circulated to the fan-coils in the air-conditioned space.

In the programed cooling system, the CTES component is sized at 3.26 m^3 (including the volume of coils) for a total storage capacity of 140 kWh. The phase change temperature of CO_2 gas hydrate (at a certain pressure) is 7ºC, the latent heat is 313 kJ/kg and specific heat is 2.48 kJ/(kg·K). The electric-driven vapour compression air-cooled chiller is sized at 25 kW to shoulder the peak load during ventilation period with a rated coefficient of performance (CoP) of 3.5. The chiller's set-point is 7ºC for the BS case. Since a sufficient temperature difference between PCM and heat transfer fluid (HTF) should be maintained for heat transfer, the chiller set-point for the CS case is 5ºC. The HTF in this study employs water.

The battery used is a lead-acid storage battery with the storage capacity of 79.2 kWh and the charging efficiency of 0.9. The PV panel uses the SPV module manufactured by Rajasthan Electronic Instrumentation Ltd Jaipur with the rated voltage of 17.0 V and the rated current of 4.12 A for each module. The PV panels are sized at a fixed area of 42.0 m^2 to cover around 65% of the total power consumption of the BS case. The rest of power consumption is to be offset by electricity grid. The battery charger and voltage regulator have an efficiency of 78%; and the DC/AC inverter is assumed to have an efficiency of 96%.

Full-storage operation mode is adopted in the system simulation, as is shown in Figure 2. In the BS case, electricity is generated by solar panels from 9:00 AM to 5:00 PM and is totally charged in a battery; during ventilation periods (6:00–9:00 AM, 5:00–10:00 PM), electricity is discharged from the battery to operate the HVAC chiller to supply cooling. In the CS case, the generated electricity is directly exploited to run the chiller to produce cooling capacity, which is stored in a CTES; during ventilation periods, cooling capacity is released from the CTES and supplied to users.

2.3 Modelling procedure

The computer model of the PV cooling system has been developed in the transient simulation software environment TRNSYS 16.1 [Thermal Energy System Specialists (TESS), 2007]. The system structure is shown in Figure 3. The constructed TRNSYS deck file is composed of a multi-zone building, a CTES and cooling supply module (an electric chiller integrated with a CTES in parallel with fan-coils), and a PV-battery electricity generation and storage module. Signals are given to control the inverter, chiller, pumps and fan according to the ventilation schedules and indoor temperature and humidity feedback.

The component of battery uses a lead-acid battery storage operating in conjunction with solar arrays and air conditioning components. It specifies how the state of charge varies over time and gives the rate of charge or discharge.

The CTES component is programmed using validated effectiveness-NTU model [9, 10]. The effectiveness, defined as a ratio of the actual discharged heat to the theoretical maximum heat that can be discharged, is found to be a function of mass flux. It describes the average NTU of the CTES, which can be presented by the average thermal resistance between HTF and PCM at the phase interface.

$$\varepsilon = 1 - exp(-NTU)$$

$$NTU = \frac{UA}{(\dot{m}C_p)} = \frac{1}{R_T \dot{m} C_p}$$

Considering the cooling coil in the CTES is a long tube surrounded by a certain volume of PCM, the total thermal resistance R_T can be expressed as

$$R_T = R_{HTF} + R_{WALL} + R_{PCM} = \frac{1}{2\pi R_i L h_{HTF}} + \frac{ln(R_o/R_i)}{2\pi k_{WALL} L} + \frac{ln[\frac{(\delta({R_{max}}^2 - {R_o}^2) + {R_o}^2)^{\frac{1}{2}}}{R_o}]}{2\pi k_{PCM} L}$$

The heat transfer between HTF and PCM can be correlated to the energy gain or loss of HTF. Consequently, the heat transfer and outlet HTF temperature can be calculated from

$$Q = \varepsilon \dot{m} C_p (T_i - T_{PCM}) = \dot{m} C_p (T_o - T_i)$$

By using the effectiveness-NTU method, a CTES component with HTF (water) flowing in the coils and PCM (CO_2 gas hydrate) freezing/melting outside the coils can be modelled.

2.4 System evaluation indices

The evaluation on energy saving performance of the single storage and the cooling system is based on some indices. Two dimensionless indices for evaluating the battery storage are the self-consumption ratio (the share of the power charged by battery (Q_{BC}) in the total produced power by PV arrays (Q_{PV})) and the self-sufficiency ratio (the ratio of the load power (Q_{LP}) to the power discharged from battery (Q_{BD})) [17]. For the coolth storage, the energy efficiency is used as an index, which is defined as the ratio of the energy output to the energy input to the CTES. Exergy analysis method gives information on the quality and quantity of energy transferred in a latent heat energy storage [18]. The output exergy equals to the difference

between the input exergy and the exergy destroyed (exergy lost due to irreversibility), and is used to evaluate the energy saving of coolth storage in this study.

Power consumption of the cooling system mainly consists of power consumed by the chiller, pumps and fans. Primary energy saving, in literature, is usually expressed as the difference between the power consumed in system operation and the energy supplied from the cooling system [19–21]. In this way, primary energy saving ratio (PESR) is defined in this study as the ratio of the cooling capacity supplied from the cooling system to the net power consumed by running the system (power consumed by chiller, pumps and fans minus power supplied by PV). The power consumption and PESR are indices to evaluate the system. The expressions of all these indices are listed in Table 2.

3 Results and discussions

By using the model, the power consumption and PESR of the cooling system using different storage approaches are predicted. The system performance during a typical summer day and during the cooling season is simulated. Besides, influencing factors of a single battery and CTES are studied in a simplified system.

3.1 Operation on a typical summer day

The variation of energy and temperature of both BS case and CS case on a typical hot sunny day in the summer of Brisbane is shown in Figure 4 and 5. In the BS case (Figure 4), the cooling supply is 89.6 kWh, and the total system electricity consumption is 69.0 kWh with the PV panels covering 42.8 kWh. The battery was charged to 98% during the day and discharged to 45% during the night, and then to 11% in the next morning. In the CS case (Figure 5), the total electricity consumption of the day is 77.7 kWh. There is 118.1 kWh cooling capacity charged and 88.9 kWh discharged. During the discharge, the temperature of the PCM does not deviate from the phase change temperature, which means both liquid phase and solid phase coexist in the CTES with the liquid fraction varying from 15.6% to 79.1%.

3.2 Operation during the cooling season

The cooling supply and power consumption of both storage cases during the cooling season under different climates are shown in Figure 6. Owing to the difference in the cooling load of different climates, both cooling supply and power consumption in Shanghai and Brisbane are larger than that in Madrid. However, since solar radiation in Shanghai is lower than that in the other two, its PV power supply is lower. The large power consumption but relatively low PV

power supply in Shanghai leads to a situation that the cooling supply is largely dependent on the electricity grid unless a larger PV panel size is adopted. In the result, based on a same PV panel size, PV power supply accounts for 56.2% for Shanghai, 68.2% for Madrid and 66.7% for Brisbane in the BS case; it accounts for 56.8% for Shanghai, 70.7% for Madrid and 61.2% for Brisbane in the CS case. This also reveals that the CS case might be more sensitive to the change of cooling load and solar radiation compared to the BS case.

In the BS case, in some cases the power output from PV cannot be collected due to the fully charged battery. In the CS case, the discharged cooling capacity from the coolth storage is obviously less than the charged, mainly owing to the heat gain during the storage period. On the other hand, there are gaps between the power consumption of the two cases, which can be attributed to three respects. The leading factor is the secondary pump used in the CS case resulting in 11% extra energy cost. Secondly, in order to enhance the heat transfer in CTES, the chilled water temperature is reduced, which may lead to a lower chiller CoP and higher energy cost. Last but not least, the coolth storage undergoes heat gain during "standby period", while battery is able to conserve electricity for a relatively long time with ignorable electricity loss. It is also admitted that the energy loss from battery is electricity at the expense of solar energy, while the energy loss from CTES is cooling capacity produced using electricity, hence it is believed that "high-grade" energy is depleted in CTES. The amount of heat gain of CTES is affected by the difference between the ambient temperature and PCM temperature.

The PESR and energy efficiency of both storage cases are obtained from Figure 6 and are shown in Figure 7. The PESR of BS case and CS case is respectively 2.8 and 1.9 times higher than that of the reference case with no storage. However, due to the reasons mentioned above, the storage efficiency of coolth storage (0.77 on average) is less than that of battery (0.89 on average). The PESR of the CS case (4.25 for Shanghai, 5.54 for Madrid and 4.24 for Brisbane on average) is also obviously less than that of the BS case (6.06 for Shanghai, 7.08 for Madrid and 7.64 for Brisbane on average). To improve energy saving of both cases, it is significant to know how energy storage performance could be influenced by the operating condition.

3.3 Performance and influencing factors on a single battery/coolth storage

In this section, the charging/discharging performance of a single battery storage and a single coolth storage is studied independent from the above mentioned system. Instead, a small-scale and simplified system is built in the simulation. PV panels with a set of two modules in series and three modules in parallel are arranged, charging a field of 24 V × 16.5 Ah batteries with three cells in parallel.

The effect of solar radiance on the charge of battery is shown in Figure 8. The charging rate and power loss rate grow proportionally with the rise of solar radiation. The self-consumption ratio also increases linearly with solar radiation until it reaches 0.9 kW/m^2; after this point, the self-consumption ratio starts to drop due to the dumped PV power. On the other hand, the charging time decreases rapidly as solar radiation increases before 0.2 kW/m^2; after this point, the decreasing rate becomes slow. It reveals that for a fixed battery size, higher solar radiation helps to improve the rate of charge to some extent, however it results in larger power loss at the same time.

The effect of load power on the discharging process of the battery is shown in Figure 9. The discharging rate rises with the increase in load power; consequently the discharging time decreases with it. On the other hand, since the power discharged from battery does not grow at a same speed with the linear growth of the load power, the self-sufficiency ratio declines from 0.89 to 0.72 as the load power rises from 0.10 kW to 0.21 kW.

The effect of HTF temperature and cooling load on the exergy output and storage efficiency of the coolth storage is illustrated based on per m^3 tank size with a rated storage capacity of 43.0 kWh. The flowrate of HTF is constant at 0.3 kg/s.

In the charging process as shown in Figure 10, the average exergy output of the coolth storage declines linearly with the growth of HTF temperature, indicating that the charging rate drops proportionally with the reduction in heat transfer temperature difference. Meanwhile, the rise in HTF temperature leads to a decline in the energy efficiency and an extended charging time (from 7.45 h to 50.5 h). It reveals that a lower HTF temperature is favourable for the energy efficiency of coolth storage; however the CoP of the chiller should also be considered.

During the discharge in Figure 11, the growth of exergy output is in direct proportion to the growth of the cooling load. Due to the increase in the cooling load, time for the completion of discharge reduces, and it leads to a decrease in the surface heat gain during the discharging period. As a consequence, the energy efficiency increases with the rise in cooling load. The deflection point is around 2.1 kWh, after which the effect of cooling load on energy efficiency and charging time becomes insignificant.

Conclusion

A simulation was conducted to compare a phase change coolth storage with a battery storage in a PV cooling system under the climate of Shanghai, Madrid and Brisbane. The performance, power consumption and primary energy saving of both energy storage approaches and their influencing factors were predicted.

The main finding of this study is that the PESR of the battery case is 2.8 times higher than that of the reference case; while the PESR of the coolth storage case is 1.9 times higher than is. This shows that under the studied climates, coolth storage could favour PV-cooling systems in terms of energy saving, however it is not comparable to battery storage. The main reason is considered to be the heat gain during the long standby period of the coolth store. It can be overcome by well-insulating the coolth store. Another reason is the relatively low efficiency of HVAC chiller in the CS case due to the low evaporating temperature used to charge the coolth store. This also reveals the importance to enhance phase change materials.

For a single storage, the charging rate and self-consumption ratio of battery are both largely affected by solar radiation. The energy efficiency of coolth storage is greatly affected by HTF temperature in the charge, and is affected to a small extent by cooling load in the discharge. These factors are key to the decision-making for which type of energy storage should be used for different climates, HVAC chiller types, building functions and cooling loads. In the future research, the initial cost of the storage installation should also be considered for the selection of a suitable energy storage approach for cooling systems.

References

[1] Renato M. Lazzarin. Solar cooling: PV or thermal? A thermodynamic and economical analysis. Int. J. Refrig.2014, 39: 38–7.

[2] Ahmer A.B. Baloch, Haitham M.S. Bahaidarah, Palanichamy Gandhidasan, et a. Experimental and numerical performance analysis of a converging channel heat exchanger for PV cooling. Energ Convers Manage 2015, 103: 14–27.

[3] Xiaolin Wang, Mike Dennis. Influencing factors on the energy saving performance of battery storage and phase change cold storage in a PV cooling system. Energ Buildings 2015, 107:84–92.

[4] Ursula Eicker, Antonio Colmenar-Santos, Lya Teran, et al. Economic evaluation of solar thermal and photovoltaic cooling systems through simulation in different climatic conditions: An analysis in three different cities in Europe. Energ Buildings 2014, 70: 207–223.

[5] Bo Lu. Short-term scheduling of battery in a grid-connected PV / battery system. IEEE transactions on power systems 2005, 20(2): 1053–1061.

[6] N. Molero-Villar, J.M. Cejudo-Lo´pez, F. Domı´nguez-Mun˜oz, et al. A comparison of solar absorption system configurations. Sol Energy 2012, 86: 242–252.

[7] Agyenim F, Knight I, Rhodes M. Design and experimental testing of the performance of an outdoor LiBr/H_2O solar thermal absorption cooling system with a cold store. Sol Energy 2010, 84(5): 735–44.

[8] X.Q. Zhai, M. Qu, Yue. Li, et al. A review for research and new design options of solar absorption cooling systems. Renew Sust Energ Rev 2011, 15: 4416–4423.

[9] N.H.S. Tay, M. Belusko, F. Bruno. Designing a PCM storage system using the effectiveness- number of transfer units method in low energy cooling of buildings. Energ Buildings 2012, 50: 234–242.

[10] N.H.S. Tay, M. Belusko, F. Bruno. An effectiveness-NTU technique for characterizing tube-in-tank phase change material energy storage systems. Appl Energ 2012, 91: 309–319.

[11] Xiaolin Wang, Mike Dennis, Liangzhuo Hou. Clathrate hydrate technology for cold storage in air conditioning systems. Renew Sust Energ Rev 2014, 36: 34–51.

[12] W. Lin, A. Delahaye, L. Fournaison. Phase equilibrium and dissociation enthalpy for semi-clathrate hydrate of CO_2 +TBAB. Fluid Phase Equilibr 2008, 264: 220–227.

[13] Wei Lin, Didier Dalmazzone, Walter Furst, et al. Thermodynamic Studies of CO_2 + TBAB + Water System: Experimental Measurements and Correlations. J Chem Eng Data 2013, 58: 2233–2239.

[14] Hiroyuki Oyama, Wataru Shimada, Takao Ebinuma, et al. Phase diagram, latent heat, and specific heat of TBAB semiclathrate hydrate crystals. Fluid Phase Equilibr 2005, 234: 131–135.

[15] Ziad Youssef, Lucian Hanu, Tobias Kappels, et al. Experimental study of single CO_2 and mixed CO_2+TBAB hydrate formation and dissociation in oil-in-water emulsion. Int J Refrig 2014, 46: 207–218.

[16] Doemland, Inga (2015). Feasibility of residential solar air-conditioning in Australia, including space heating and hot water (Doctoral dissertation).

[17] Johannes Weniger, Tjarko Tjaden, Volker Quaschning. Sizing of residential PV battery systems. Energy Procedia 2014, 46: 78–87.

[18] Ahmet Koca, Hakan F. Oztop, Tansel Koyun, et al. Energy and exergy analysis of a latent heat storage system with phase change material for a solar collector. Renew Energ 2008, 33: 567–574.

[19] F. Calise, A. Palombo, L. Vanoli. Maximization of primary energy savings of solar heating and cooling systems by transient simulations and computer design of experiments. Appl Energ 2010, 87: 524–540.

[20] Dan Staniaszek, Eoin Lees. Determining energy savings for energy efficiency obligation schemes. The Regulatory Assistance Project 2012

[21] B. Rismanchi, R. Saidur, G. BoroumandJazi, et al. Energy, exergy and environmental analysis of cold thermal energy storage (CTES) systems. Renew Sust Energ Rev 2012, 16: 5741–5746.

[22] Ibrahim Dincer. On thermal energy storage systems and applications in buildings. Energ Buildings 2002, 34:377–388.

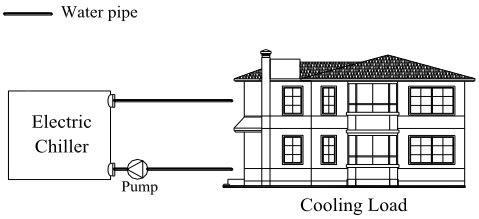

(a) Electric cooling – reference case

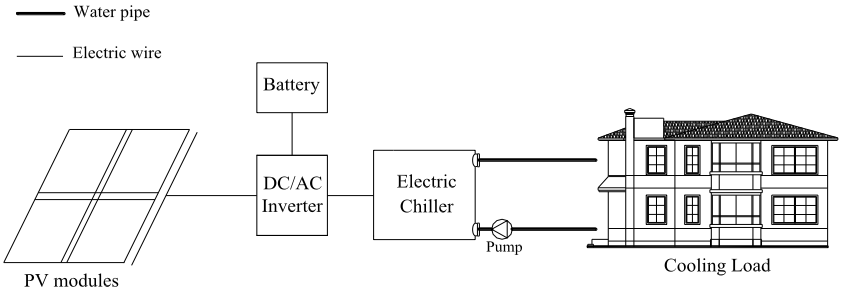

(b) PV cooling – battery storage case

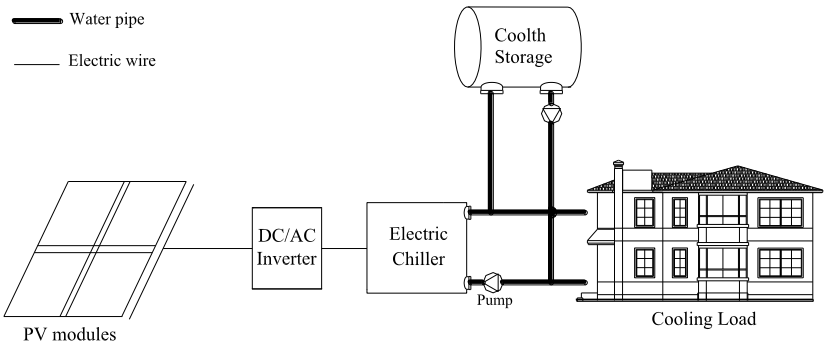

(c) PV cooling – coolth storage case

Figure 1 Different configurations of the cooling system

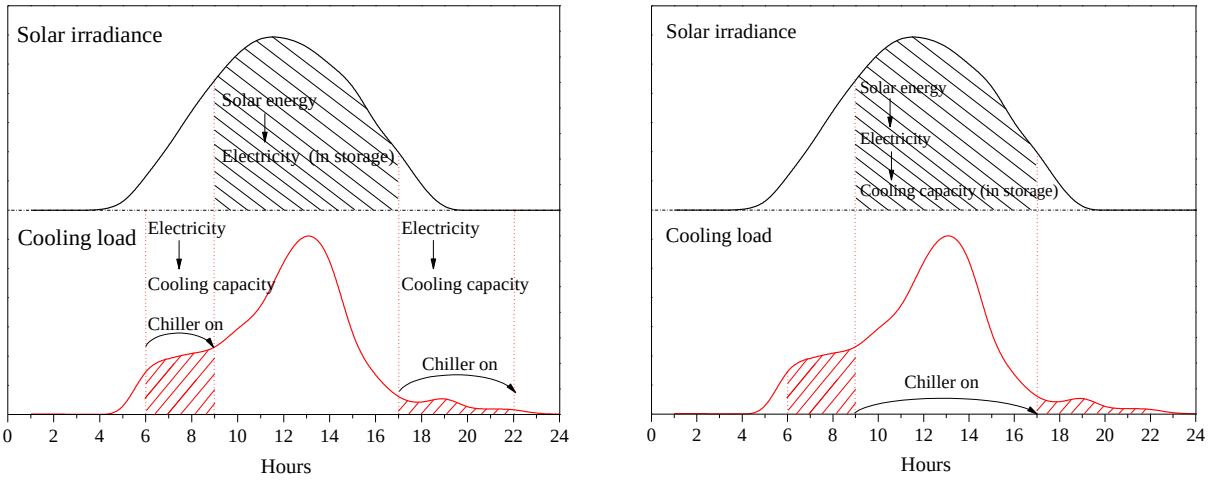

(a) battery storage case (b) coolth storage case

Figure 2 Energy flow chart of full-storage operating strategy

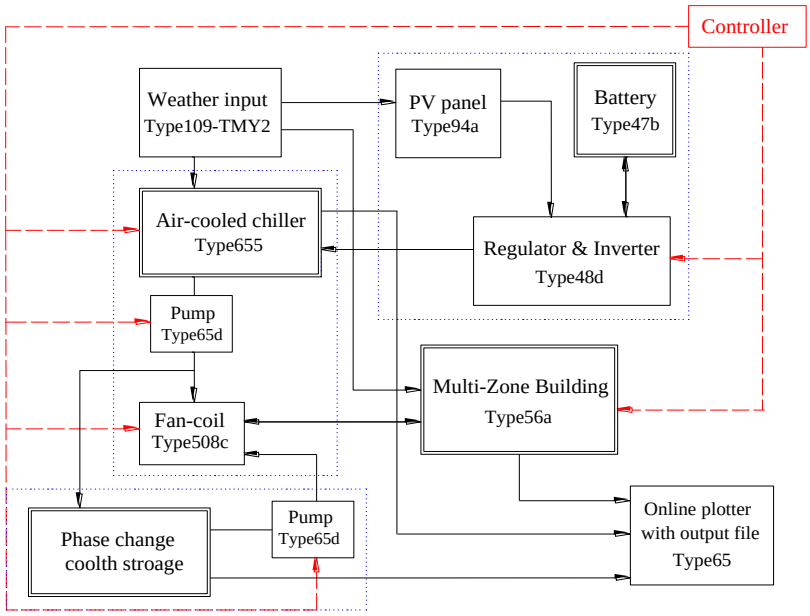

Figure 3 TRNSYS diagram of the cooling system

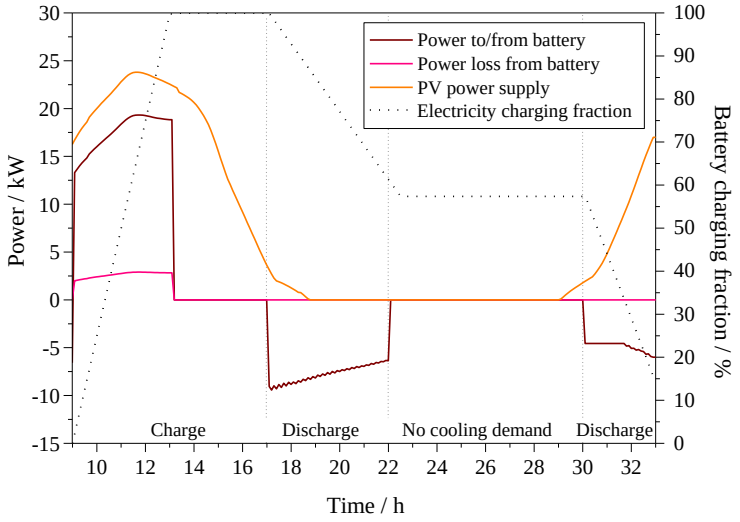

(a) Battery power and battery charging fraction

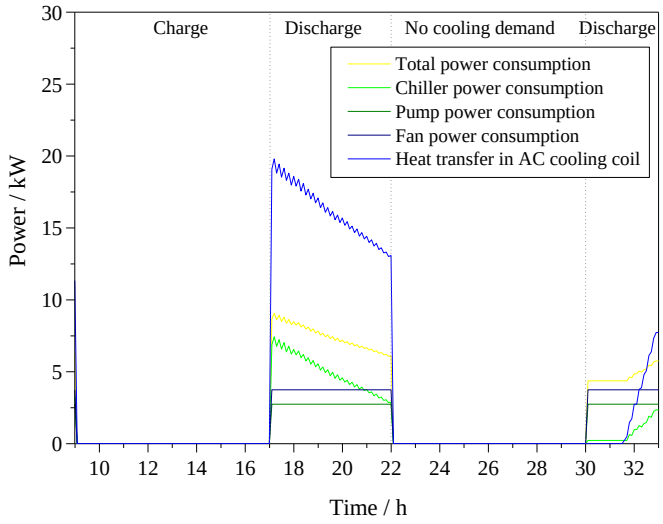

(b) Power consumption and cooling supply

Figure 4 Energy change of battery case on a typical summer day

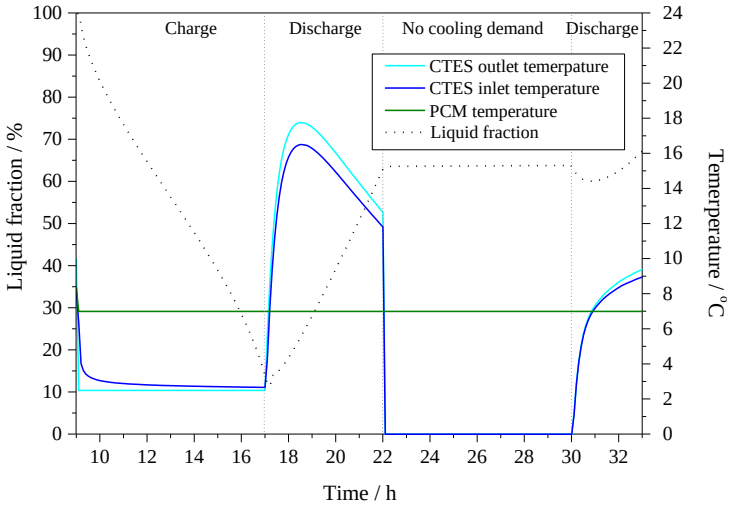

(a) Temperature and liquid fraction

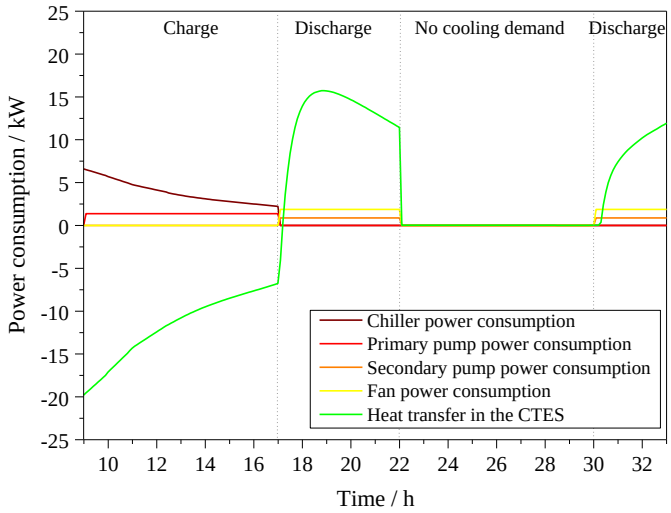

(b) Power consumption and cooling supply

Figure 5 Energy and temperature variation of coolth storage case on a typical summer day

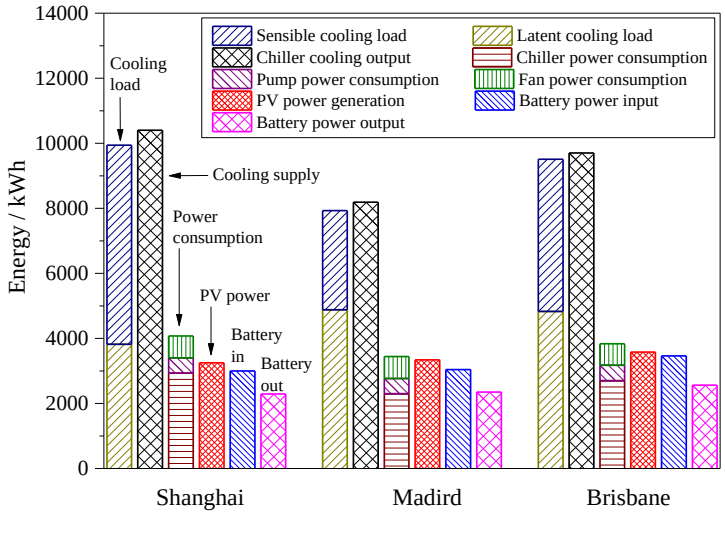

\

(a) Battery storage case

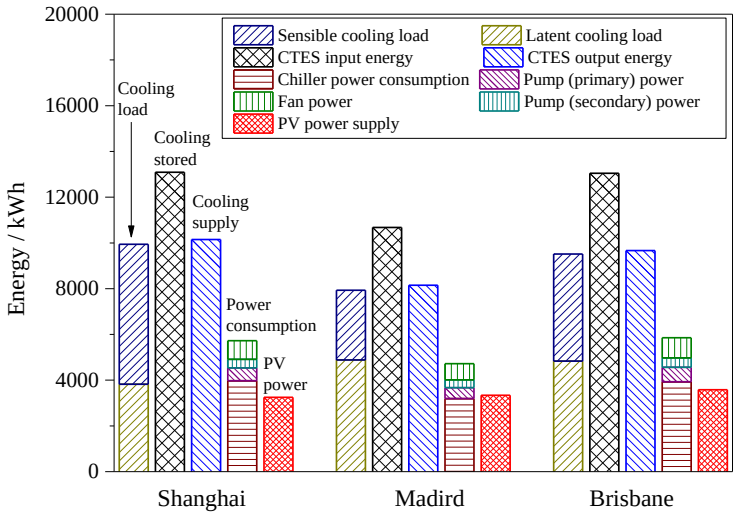

(b) Coolth storage case

Figure 6 Cooling season power consumption of both cases under different climates

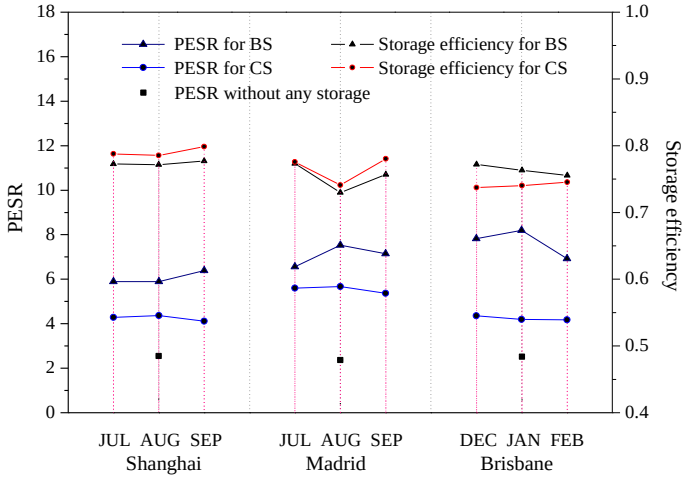

Figure 7 PESR and storage efficiency of both cases under different climates

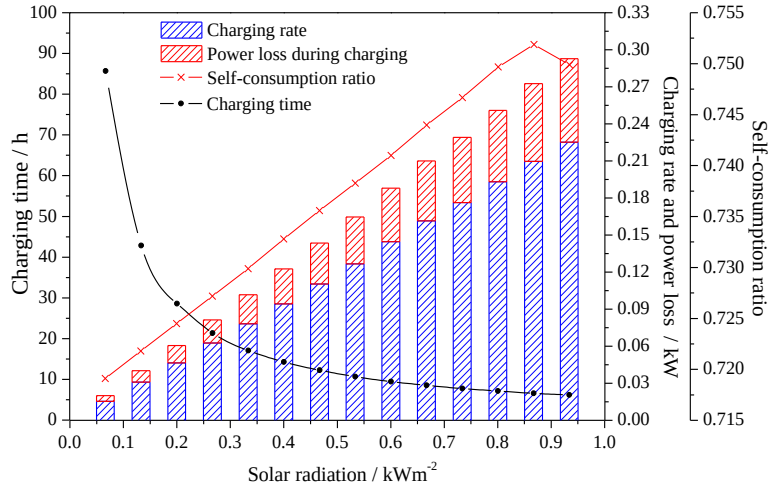

Figure 8 Charging performance of battery under different solar radiation

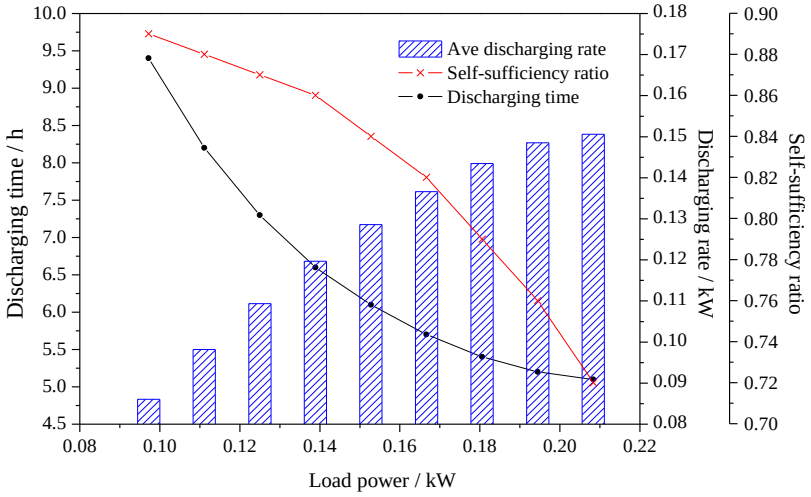

Figure 9 Discharging performance of battery under different load power

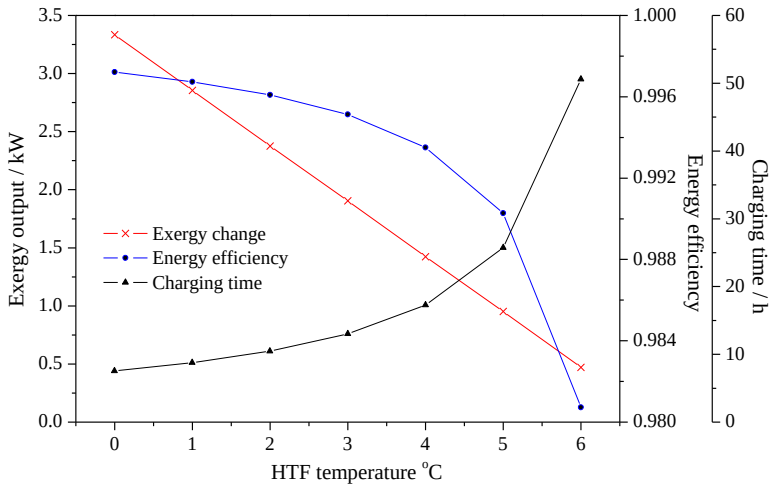

Figure 10 Charging performance of coolth storage at different HTF temperature

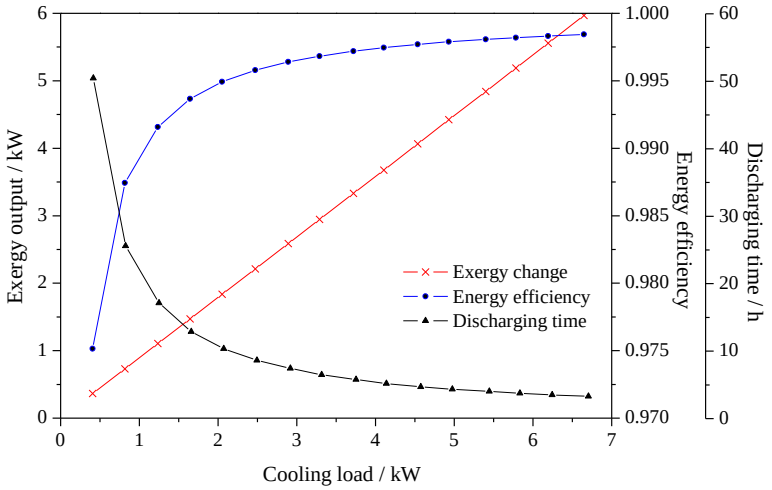

Figure 11 Discharging performance of coolth storage under different cooling load

Table 2 Expressions of system evaluation indices

Object	Index	Expression	Reference
Battery	Self-consumption ratio	$r_c = Q_{BC} / Q_{PV}$	[17]
	Self-sufficiency ratio	$r_s = Q_{BD} / Q_{LP}$	
Coolth storage	Storage energy efficiency	$\eta_{CS} = \frac{Q_o}{Q_i} = \frac{Q_i - Q_r}{Q_i}$	[18,22]
	Exergy output	$\Delta A = A_o - A_i = \dot{m} C_p [(T_o - T_i) - T_{amb} ln(\frac{T_o}{T_i})]$	[22]
System	Power consumption	$Q_{Cons} = Q_{ELEC\_CHILLER} + Q_{ELEC\_PUMP} + Q_{ELEC\_FAN}$	/
	Primary energy saving ratio	$PESR = \frac{Q_{Output}}{Q_{Input}} = \frac{Q_{Energy\ supply\ from\ cooling\ coil}}{Q_{Power\ consumed} - Q_{Power\ from\ PV}}$	/

Table 1 Parameters and schedules for the simulated multi-zone building

Zones	Living room	Bedroom 1	Bedroom 2	Bedroom 3
Area	90 m^2	30.5 m^2	35.6 m^2	40 m^2
Internal gain (equipment)	1100 W (cooking)	300 W	300 W	530 W (a computer)
Internal gain (lighting)	449.5 W	152.5 W	177.8 W	200 W
Occupation rate	0.1	0.03	0.03	0.03